Rare Earth Arylsilazido Compounds with Inequivalent Secondary Interactions

ChemComm

Rare Earth Arylsilazido Compounds with Inequivalent Secondary Interactions†‡

Kasuni C. Boteju,[a] Suchen Wan,[b] Amrit Venkatesh,[a] Arkady Ellern,[c] Aaron J. Rossini[a] and Aaron D. Sadow*[a]

A new bulky silazido ligand, –N(SiHMe₂)Dipp (Dipp = C₆H₃-2,6-iPr₂) supports planar, three-coordinate homoleptic rare earth complexes Ln{N(SiHMe₂)Dipp}₃ (Ln = Sc, Y, Lu) that each contain three secondary Ln←HSi interactions and one agostic CH bond. Y{N(SiHMe₂)Dipp}₃ and acetophenone react via hydrosilylation, rather than by insertion into the Y–N bond or enolate formation.

The hexamethyl disilazido group's use as a ligand in homoleptic and heteroleptic complexes, which find myriad synthetic applications, spans the periodic table.[1] This ligand is particularly useful in early metal and lanthanide chemistry because its steric properties lead to monomeric, reactive species. Interestingly, solid-state structures of trivalent lanthanide compounds Ln{N(SiMe₃)₂}₃ are pyramidalized (Σ_{NLnN} = 339–353°),[2] whereas smaller M{N(SiMe₃)₂}₃ (M = Ti, V, Cr, Fe, Al, Ga, In) are planar.[3] The scandium compound Sc{N(SiMe₃)₂}₃ is planar in the gas-phase[4] but pyramidal in the solid state. These compounds, as well as those supported by the less hindered tetramethyldisilazido, contain secondary interactions of the type Ln←RSi (R = Me, H) with groups beta to the metal center;[5,6,7] however, these interactions are not sufficient to prevent additional solvent coordination or dimerization in homoleptic tetramethyldisilazido rare earth compounds.[5,8] Indirect, but compelling, evidence for the existence of Ln←HSi interactions is provided by distorted ligand conformations in X-ray diffraction studies, reduced one-bond coupling constants ($^1J_{SiH}$) in NMR spectra, or low energy Si-H stretching modes (ν_{SiH}) in infrared spectra.[5,6] Bulkier disilazido ligands N(SitBuMe₂)SiMe₃ or N(SitBuMe₂)₂ form planar homoleptic lanthanide compounds.[9]

The bulky silazido ligand N(SiMe₃)Dipp (Dipp = 2,6-diisopropylphenyl) supports homoleptic divalent first row metal centers,[10] and heteroleptic and homoleptic rare earth species, such as LuCl{N(SiMe₃)Dipp}₂THF and La{N(SiMe₃)Dipp}₃.[11,12] The latter compound adopts a pyramidal geometry at La (Σ_{NLaN} = 337°). Less bulky aryl substitution also gives THF-coordinated or "ate"-type rare earth compounds, including Ln{N(SiMe₃)Ph}₃THF (Ln = Y, Lu),[11] and [YCl{N(SiMe₃)2,6-C₆H₃Et₂}₃][Li(THF)₄].[13] Alternatively, a combination of the large tBu and the small, β-SiH-containing SiHMe₂ substituents in a silazido provides homoleptic Ln{N(SiHMe₂)tBu}₃ (Ln = Sc, Y, Lu, Er).[14,15] Ln{N(SiHMe₂)tBu}₃ form pyramidal structures akin to Ln{N(SiMe₃)₂}₃, contain three bridging Ln←HSi in a C_3-symmetric structure, and will coordinate THF or Et₂O. The SiH group in N(SiHMe₂)tBu is reactive. For example, Cp₂Zr{N(SiHMe₂)tBu}X compounds react by H abstraction of the silicon hydride.[16] The combination of an even larger substituent than tBu with the small SiHMe₂ could result in further SiH bond activation by pushing the smaller group closer to the metal center. To explore this idea, we constructed N(SiHMe₂)Dipp as a sterically off-balanced ligand.

The synthesis of HN(SiHMe₂)Dipp is modified from that of HN(SiMe₃)Dipp.[17] Deprotonation of H₂NDipp by nBuLi in pentane generates LiN(H)Dipp as a white precipitate. This crude material and Me₂HSiCl react in diethyl ether to provide HN(SiHMe₂)Dipp (**1**; eqn (1)), which is isolated in good yield.

$$\text{H}_2\text{NDipp} \xrightarrow[\substack{\text{pentane} \\ 0\,°C\ \text{to r.t., 12 h}}]{n\text{BuLi}} \text{LiN(H)Dipp} \xrightarrow[\substack{\text{Et}_2\text{O} \\ 0\,°C\ \text{to r.t., 3 h}}]{\text{Me}_2\text{HSiCl}} \mathbf{1},\ 83.3\% \qquad (1)$$
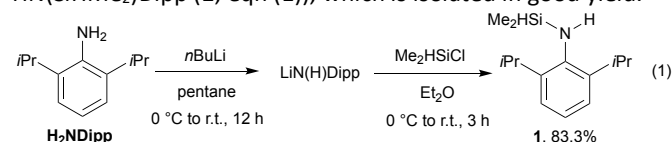
Deprotonation of **1** with nBuLi in pentane gives the desired lithium silazido LiN(SiHMe₂)Dipp (**2**; eqn (2)) as a white solid. Recrystallization from a saturated pentane solution at –30 °C provides analytically pure crystalline material. The ¹H NMR spectra of **1** and **2** contained resonances at 4.89 ppm ($^1J_{SiH}$ = 199 Hz) and 5.09 ppm ($^1J_{SiH}$ = 177 Hz), respectively, assigned to the

a. Department of Chemistry and US DOE Ames Laboratory, 1605 Gilman Hall, Iowa State University, Ames IA 50011, USA
b. College of Chemistry, Beijing Normal University, No.19, XinJieKouWai St., HaiDian District, Beijing 100875, P. R. China
c. Department of Chemistry, 1605 Gilman Hall, Iowa State University, Ames IA 50011, USA

SiH groups. The higher frequency chemical shift (δ_{SiH}) of **2**, with respect to silazane **1**, contrasts the lower δ_{SiH} in LiN(SiHMe$_2$)$_2$ and LiN(SiHMe$_2$)tBu compared to their silazanes (Table 1). The IR spectra for **1** and **2** revealed signals at 2112 cm^{-1} and 2022 cm^{-1}, respectively, that were assigned to v_{SiH}.

$$Me_2HSi \underset{\underset{iPr}{\bigcirc}}{\overset{N \diagdown H}{\text{—}}} iPr \xrightarrow[\substack{pentane \\ -78\ °C\ to\ r.t.,\ 12\ h}]{nBuLi} Li \underset{\underset{iPr}{\bigcirc}}{\overset{N \diagdown SiHMe_2}{\text{—}}} iPr \quad (2)$$

1   **2**, 97.2%
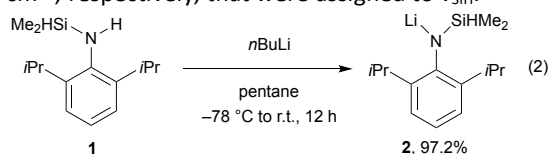
Table 1. Room temperature ^{1}H NMR (in benzene-d_6) and IR spectroscopic properties of SiH groups in silazanes, disilazanes, lithium silazido, and rare earth silazido compounds.

Compound	δ_{SiH} (ppm)	$^1J_{SiH}$ (Hz)	v_{SiH} (cm^{-1})
HN(SiHMe$_2$)Dipp (**1**)	4.89	199	2112
LiN(SiHMe$_2$)Dipp (**2**)	5.09	177	2022
HN(SiHMe$_2$)$_2$^{a}	4.82	170	2120
LiN(SiHMe$_2$)$_2$^{a}	4.49	168	1990
HN(SiHMe$_2$)tBu^b	4.82	192	2135 and 2104
LiN(SiHMe$_2$)tBu^b	4.49	168	2052
Sc{N(SiHMe$_2$)Dipp}$_3$ (**3**)	5.43	143	2105, 2046, 1908
Y{N(SiHMe$_2$)Dipp}$_3$ (**4**)	5.17	129	2107, 1934, 1883
Lu{N(SiHMe$_2$)Dipp}$_3$ (**5**)	5.43	128	2108, 1942, 1877

^{a}See reference 5; ^{b}See references 15, 18.

Salt metathesis reactions of LnCl$_3$THF$_n$ and **2** (3 equiv.) provide the homoleptic tris(silazido) rare earth compounds Ln{N(SiHMe$_2$)Dipp}$_3$ (Ln = Sc (**3**), Y (**4**), Lu (**5**); eqn (3)).

$$\begin{array}{c} LnCl_3(THF)_n \\ + \\ 3\ LiN(SiHMe_2)Dipp \end{array} \xrightarrow[\substack{-78\ °C\ to\ r.t. \\ 12\ h}]{Et_2O} \quad \text{[structure]} \quad (3)$$

Ln = Sc; n = 3
Y, Lu; n = 0

Ln = Sc **3**, 43.2%; Y **4**, 56.2%; Lu **5**, 45.5%
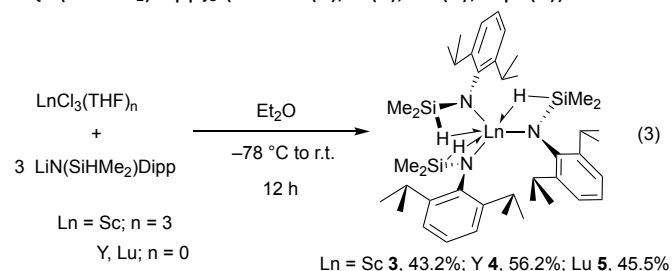
The reactions proceed in diethyl ether at low temperature, and the products are isolated as donor-free and salt-free crystalline materials after extraction and crystallization from pentane. Their ^{1}H NMR spectra, measured at room temperature in benzene-d_6, revealed one set of N(SiHMe$_2$)Dipp resonances. The isopropyl groups appeared as a well-resolved doublet and a septet in each spectrum of **3** – **5**, indicating that the Dipp group rapidly rotates around the N–C bond at room temperature. The SiH signal appeared as a broad singlet in **3**, but the spectra of **4** and **5** contained the expected septet splitting pattern.

The room temperature δ_{SiH} for **3** – **5** were even higher than the corresponding values in the lithium silazido starting material **2** (Table 1), and $^1J_{SiH}$ values were also significantly reduced (143 – 128 Hz). We noticed, however, that the $^1J_{SiH}$ values in **3** – **5** were larger than those in the related series Ln{N(SiHMe$_2$)tBu}$_3$ (Ln = Sc, 125 Hz; Y, 124 Hz; Lu 121 Hz). The chemical shifts and coupling constants of the latter compounds' three bridging Ln←HSi groups are temperature independent to 200 K.[15]

In contrast to Ln{N(SiHMe$_2$)tBu}$_3$, **3** – **5** are fluxional; moreover, the low temperature NMR spectra suggest a low

symmetry structure with three unique N(SiHMe$_2$)Dipp ligands. For example, the ^{1}H NMR spectrum of **4** at 205 K in toluene-d_8 (Figure 1) contained δ_{SiH} at 5.41 ppm ($^1J_{SiH}$ = 132 Hz), 5.26 ppm ($^1J_{SiH}$ = 141 Hz) and 4.89 ppm ($^1J_{SiH}$ = 116 Hz). In addition, the Dipp signals in the ^{1}H NMR spectra indicated that their rotation slowed at low temperature. The ^{1}H NMR spectrum of **4** at 205 K in toluene-d_8 contained six well-resolved resonances from 4.17 ppm to 2.34 ppm (1 H each) and twelve, partly overlapping resonances (1.63 ppm – 0.65 ppm) assigned to the methine and methyl moieties in the three distinct Dipp groups.
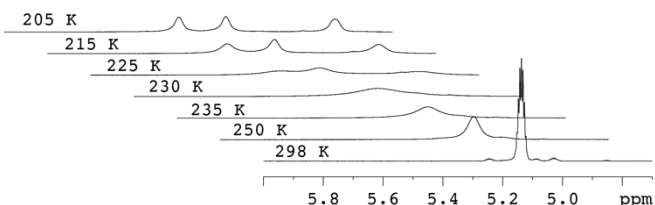
Figure 1. SiH region of ^{1}H NMR spectra of **4** acquired in toluene-d_8 from 298 to 205 K.

A 2D ^{1}H-^{89}Y HSQC spectrum (Figure 2A), acquired at 205 K in toluene-d_8, showed correlations between the three SiH signals and the ^{89}Y NMR signal at 378.5 ppm. The cross-peaks reveal inequivalent through-bond interactions between yttrium and the three bridging SiH moieties. The intensity of the cross-peaks is directly proportional to the strength of the ^{1}H-^{89}Y J-coupling, thus the most upfield ^{1}H NMR signal with the lowest $^1J_{SiH}$ value most strongly couples with the yttrium center. Note that although the ^{1}H T_2 also affects HSQC peak intensity, the three SiH groups have similar T_2 values.

The ^{29}Si NMR signal for **4** at room temperature appeared at –28.2 ppm, and this signal split at 205 K into three that ranged from only –29.4 to –30.2 ppm. In addition, the most upfield ^{1}H NMR signal at 4.89 ppm correlated to the middle ^{29}Si NMR signal at –29.6 ppm. These data suggest that the differences in Ln←HSi between the three N(SiHMe$_2$)Dipp ligands have minimal effect on the silicon centers.

Three bands in the IR spectra of **3**, **4** and **5** in the v_{SiH} region (KBr pellet; Table 1) indicate that the three N(SiHMe$_2$)Dipp ligands are also inequivalent in the solid state. This result is consistent with the solution phase structures measured by NMR spectroscopy at low temperature. Interestingly, the lowest frequency band in each compound is sharpest.

Recrystallizations of **3** – **5** from pentane provide X-ray quality crystals.‡ Interesting crystallographic features of these similarly structured molecules include trigonal planar LnN$_3$ cores, low symmetry, and short Ln–H interatomic distances. First, the trigonal planar LnN$_3$ coordination geometry (see Figure 3 and ESI) contrast the pyramidal geometries of Ln{N(SiMe$_3$)$_2$}$_3$[2] and Ln{N(SiHMe$_2$)tBu}$_3$.[14, 15] We have recently described solid state structures of alkyl compounds containing SiHMe$_2$ moieties and aryl groups, and these also give planar LnC$_3$ geometries.[19] Second, the three ligands are not related by crystallographic- or pseudo-symmetry elements in Ln{N(SiHMe$_2$)Dipp}$_3$. Two of the Dipp groups are located on one side of the LnN$_3$ plane, whereas the third Dipp is on the other side of the LnN$_3$ plane. In contrast, La{N(SiMe$_3$)Dipp}$_3$,[12]
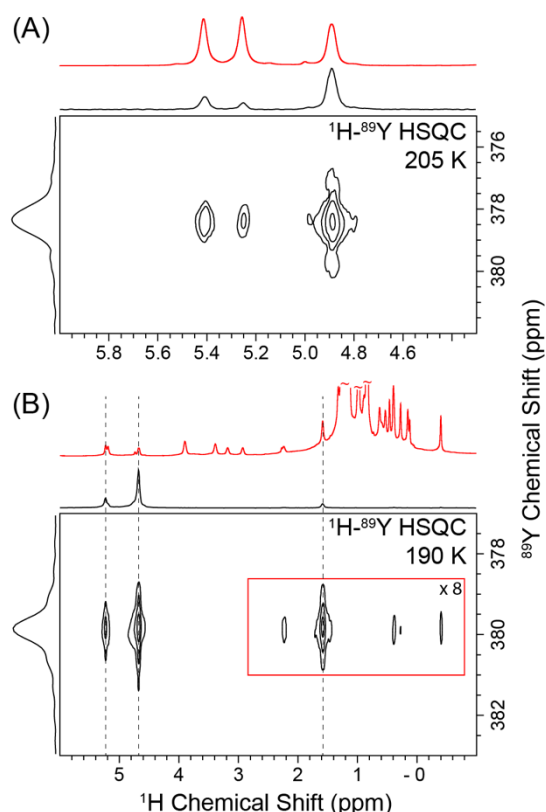
ChemComm

Figure 2. ^{1}H-^{89}Y HSQC NMR spectra of **4** acquired at (A) 205 K in toluene-d_8 and (B) 190 K in pentane-d_{12}. 1D ^{1}H NMR spectra (red) are overlaid above the ^{1}H projections of the 2D spectra.
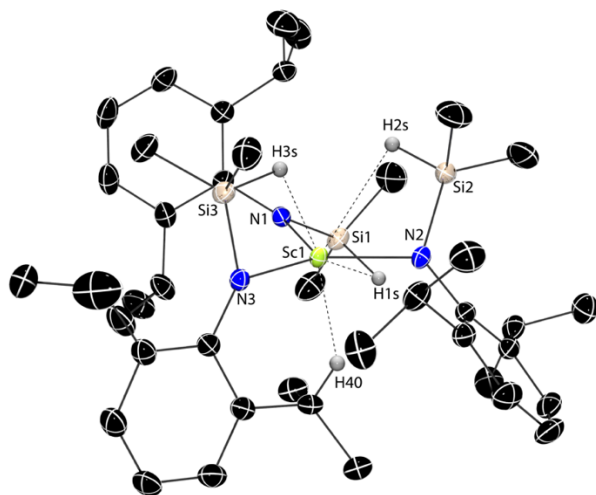
Figure 3. Rendered thermal ellipsoid plot of Sc{N(SiHMe$_2$)Dipp}$_3$ (**3**) with ellipsoids represented at 50% probability. One of two crystallographically independent molecules is illustrated (see ESI), and the H atoms included in the image are <3 Å from the Sc1 center, are located objectively and included in the refinement.

Ln{N(SiHMe$_2$)tBu}$_3$ and Ln{N(SiMe$_2$$t$Bu)SiMe$_3$}$_3$ form pseudo-C_3 symmetric molecules.[9, 14, 15] The inequivalence of the N(SiHMe$_2$)Dipp ligands extends to their interactions with the metal center. In **3** for example, the Sc1–N3 distance (2.124(2) Å) is significantly longer than Sc1–N1 and Sc1–N2 (2.089(2) and 2.098(2) Å). The non-classical Sc←HSi interactions, as characterized by the Sc–H interatomic distances (H atoms

bonded to Si are located objectively and refined) and ∠Sc–N–Si (94 – 105°), and Sc–N–Si–H torsion angles (2.6 – 9.8°) are all consistent with Sc←HSi interactions and also are all inequivalent. In particular, the Sc1–H3s distance of 2.05(2) Å is considerably shorter than the Sc1–H1s and Sc1–H2s distances (2.47(2) and 2.56(2) Å, respectively).

Remarkably, the H40 bonded to the methine of one isopropyl group, also approaches the scandium center with a very short distance (Sc1-H40, 2.34(3) Å) and suggests an agostic Sc←HC interaction. At this point, we re-examined the ^{1}H-^{89}Y HSQC spectrum to look for additional correlations; however, at 205 K, no cross-peaks were observed. Instead, the ^{1}H-^{89}Y HSQC NMR spectrum acquired at 190 K in pentane showed weak correlations between ^{89}Y and the methine and methyl signals at 2.24 and 1.59 ppm, respectively (Figure 2B).

The reaction of **4** and one equiv. of acetophenone in benzene-d_6 instantaneously provides the product Y{N(SiMe$_2$OCHMePh)Dipp}{N(SiHMe$_2$)Dipp}$_2$ (**6**) resulting from hydrosilylation of the ketone by one of the SiH groups (eqn (4)).
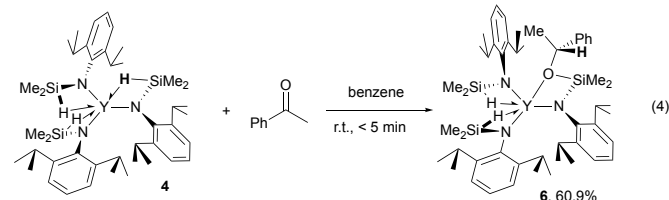
The ^{1}H NMR spectrum of **6** at room temperature showed one peak at 5.33 ppm (2 H, $^1J_{SiH}$ = 136 Hz). A new quartet and doublet at 5.0 and 1.42 ppm, which correlated in a COSY experiment, were assigned to the CHMe that resulted from acetophenone insertion into one of the SiH in **4**. These signals also correlated in ^{1}H-^{13}C HMQC and HMBC experiments with a ^{13}C NMR signal at 77.5 ppm assigned to the carbon bonded to oxygen. A ^{1}H NMR spectrum of **6** acquired at 205 K contained two resonances at 5.55 ppm ($^1J_{SiH}$ = 133 Hz) and 5.11 ppm ($^1J_{SiH}$ = 124 Hz) assigned to the SiH in inequivalent N(SiHMe$_2$)Dipp ligands. These coupling constant values indicate that two non-classical interactions Y←HSi are present in compound **6**. The IR data also showed two ν$_{SiH}$ bands at 1997 cm^{-1} and 1891 cm^{-1}. An X-ray single crystal diffraction study on **6** confirms that acetophenone has inserted into one of the SiH groups (Figure 4).$^∈$ The structural features of **6** also include a planar YN$_3$ core and short Ln–H distances (2.43(3) and 2.48(3) Å) indicative of two Y←HSi interactions.

In contrast, mixtures of the silazane HN(SiHMe$_2$)Dipp and acetophenone contain only starting materials after 1.5 d at room temperature in benzene-d_6. In addition, the lithium silazido, which reacts with acetophenone in benzene-d_6 to provide HN(SiHMe$_2$)Dipp and the lithium enolate. Related reactions of [Cp$_2$ZrN(SiHMe$_2$)$_2$]$^+$ and formaldehyde or acetone afford double addition products [Cp$_2$ZrN(SiMe$_2$OR)$_2$]$^+$ (R = Me, iC$_3$H$_7$).[20] Lanthanide-catalyzed hydrosilylations of carbonyl compounds are uncommon,[21] although we recently reported a cerium-catalyzed hydrosilylation of acrylates that provides α-silyl esters.[22] In the present case, attempts to add more than one equivalent of acetophenone to **4** provided multiple, unidentified products.
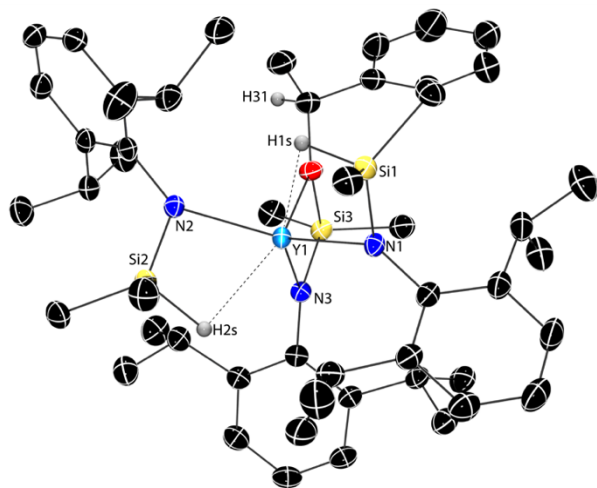
Figure 4. Thermal ellipsoid plot of Y{N(SiMe$_2$OCHMePh)Dipp}{N(SiHMe$_2$)Dipp}$_2$ (**6**). H atoms bonded to Si were located in the Fourier difference map, refined, and are included in the illustration. H31, which was placed in a calculated position, is included in the image. All other H atoms, crystallographically independent **6**, and pentane are not shown for clarity.

Thus, one of three Y←HSi secondary interactions in **4** reacts inequivalently than the other two. Here, we note that the Y←HSi moiety with the lowest δ_{SiH} and smallest $^1J_{SiH}$ also shows the greatest ^{1}H-^{89}Y HSQC peak intensity. The latter measurement probes through-bond interactions (*J*) and it is tempting to assign this group as the most activated and reactive toward hydrosilylation; however, the covalent contribution may be a small component to the overall bonding in Ln←HSi interactions. In this context, we are currently studying the reactions of **3** − **5** with other electrophiles, including more hindered ketones, to identify which SiH group reacts.

Conflicts of interest

There are no conflicts to declare.

Notes and references

✝ X-ray data for Sc{N(SiHMe$_2$)Dipp}$_3$ (**3**) (CCDC 1838231): C$_{42}$H$_{72}$N$_3$ScSi$_3$; FW 748.25; monoclinic; *a*: 12.3546(5), *b*: 20.087(1), *c*: 35.984(2), β = 90.113(2), volume: 8929.9(7); P2$_1$/c; *Z* = 8; temp. 173 K; reflections: collected, 380 031; independent, 20 360; R_{int} 0.1121; 17 130 data *I* > 2σ(*I*): R_1 0.0456, wR_2 0.0935; R_{all}: R_1 0.0689, wR_2 0.1038.
∈ X-ray data for Y{N(Si(OCHMePh)Me$_2$)Dipp}{N(SiHMe$_2$)Dipp}$_2$ (**6**) (CCDC 1838232): C$_{50}$H$_{80}$N$_3$O$_1$Si$_3$Y$_1$,3(C$_5$H$_{12}$); FW 1020.56; monoclinic; *a*: 18.7125(3), *b*: 31.0400(6), *c*: 20.6586(4), β = 93.071(1), volume: 11982.0(4); P2$_1$/n; *Z* = 8; temp. 173 K; reflections: collected, 241 230; independent, 20 073; R_{int} 0.0861;

16 158 data *I* > 2σ(*I*): R_1 0.0387, wR_2 0.0948; R_{all}: R_1 0.0542, wR_2 0.1041.

1. M. Lappert, A. Protchenko, P. Power and A. Seeber, *Metal Amide Chemistry*, John Wiley, New York, 2008.
2. R. Anwander, in *Organolanthoid Chemistry: Synthesis, Structure, Catalysis*, Springer Berlin Heidelberg, Berlin, Heidelberg, 1996, pp. 33-112.
3. P. G. Eller, D. C. Bradley, M. B. Hursthouse and D. W. Meek, *Coord. Chem. Rev.*, 1977, **24**, 1-95.
4. T. Fjeldberg and R. A. Andersen, *J. Mol. Struct.*, 1985, **128**, 49-57.
5. R. Anwander, O. Runte, J. Eppinger, G. Gerstberger, E. Herdtweck and M. Spiegler, *J. Chem. Soc. Dalton Trans.*, 1998, 847-858.
6. M. P. Conley, G. Lapadula, K. Sanders, D. Gajan, A. Lesage, I. del Rosal, L. Maron, W. W. Lukens, C. Copéret and R. A. Andersen, *J. Am. Chem. Soc.*, 2016, **138**, 3831-3843; J. Eppinger, M. Spiegler, W. Hieringer, W. A. Herrmann and R. Anwander, *J. Am. Chem. Soc.*, 2000, **122**, 3080-3096; T. D. Tilley, R. A. Andersen and A. Zalkin, *Inorg. Chem.*, 1984, **23**, 2271-2276.
7. W. A. Herrmann, R. Anwander, F. C. Munck, W. Scherer, V. Dufaud, N. W. Huber and G. R. J. Artus, *Z. Naturforsch., B: Chem. Sci.*, 1994, **49**, 1789-1797.
8. H. F. Yuen and T. J. Marks, *Organometallics*, 2009, **28**, 2423-2440.
9. C. A. P. Goodwin, K. C. Joslin, S. J. Lockyer, A. Formanuik, G. A. Morris, F. Ortu, I. J. Vitorica-Yrezabal and D. P. Mills, *Organometallics*, 2015, **34**, 2314-2325.
10. C.-Y. Lin, J.-D. Guo, J. C. Fettinger, S. Nagase, F. Grandjean, G. J. Long, N. F. Chilton and P. P. Power, *Inorg. Chem.*, 2013, **52**, 13584-13593; I. C. Cai, M. I. Lipschutz and T. D. Tilley, *Chem. Commun.*, 2014, **50**, 13062-13065.
11. H. Schumann, J. Winterfeld, E. C. E. Rosenthal, H. Hemling and L. Esser, *Z. Anorg. Allg. Chem.*, 1995, **621**, 122-130.
12. M. Visseaux, M. Terrier, A. Mortreux and P. Roussel, *Eur. J. Inorg. Chem.*, 2010, 2867-2876.
13. S.-w. Wang, H.-m. Qian, W. Yao, L.-j. Zhang, S.-l. Zhou, G.-s. Yang, X.-c. Zhu, J.-x. Fan, Y.-y. Liu, G.-d. Chen and H.-b. Song, *Polyhedron*, 2008, **27**, 2757-2764.
14. W. S. J. Rees, O. Just, H. Schumann and R. Weimann, *Angew. Chem. Int. Ed. Engl.*, 1996, **35**, 419-422.
15. N. Eedugurala, Z. Wang, K. Yan, K. C. Boteju, U. Chaudhary, T. Kobayashi, A. Ellern, I. I. Slowing, M. Pruski and A. D. Sadow, *Organometallics*, 2017, **36**, 1142-1153.
16. L. J. Procopio, P. J. Carroll and D. H. Berry, *J. Am. Chem. Soc.*, 1991, **113**, 1870-1872; L. J. Procopio, P. J. Carroll and D. H. Berry, *J. Am. Chem. Soc.*, 1994, **116**, 177-185.
17. Y. W. Chao, P. A. Wexler and D. E. Wigley, *Inorg. Chem.*, 1989, **28**, 3860-3868.
18. G. H. Wiseman, D. R. Wheeler and D. Seyferth, *Organometallics*, 1986, **5**, 146-152.
19. K. C. Boteju, A. Ellern and A. D. Sadow, *Chem. Commun.*, 2017, **53**, 716-719; A. Pindwal, K. Yan, S. Patnaik, B. M. Schmidt, A. Ellern, I. I. Slowing, C. Bae and A. D. Sadow, *J. Am. Chem. Soc.*, 2017, **139**, 16862-16874.
20. K. Yan, J. J. D. Heredia, A. Ellern, M. S. Gordon and A. D. Sadow, *J. Am. Chem. Soc.*, 2013, **135**, 15225-15237.
21. A. K. Roy, in *Adv. Organomet. Chem.*, eds. R. West, A. F. Hill and M. J. Fink, Academic Press, 2007, vol. 55, pp. 1-59.
22. A. Pindwal, S. Patnaik, W. C. Everett, A. Ellern, T. L. Windus and A. D. Sadow, *Angew. Chem. Int. Ed.*, 2017, **56**, 628-631.

ChemComm

205 K
215 K
225 K
230 K
235 K
250 K
298 K
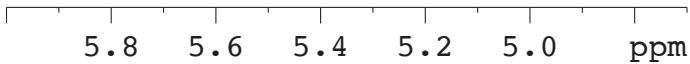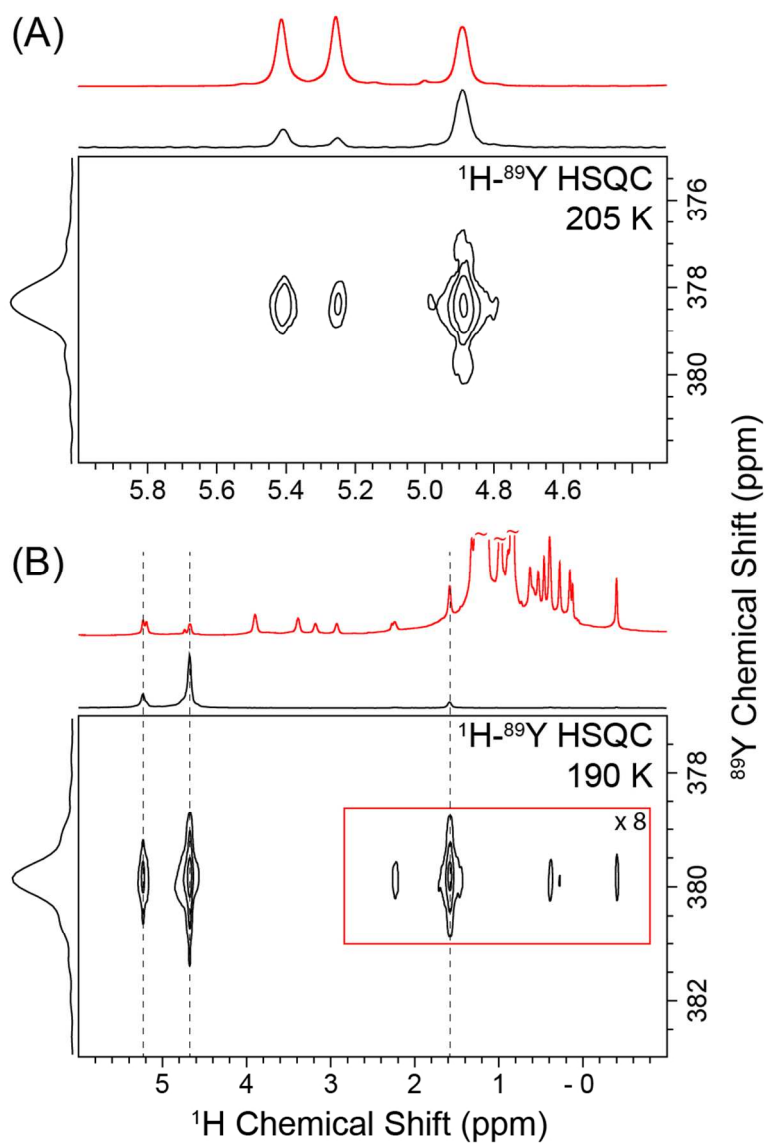
5.8   5.6   5.4   5.2   5.0   ppm

Figure 2. 1H-89Y HSQC NMR spectra of 4 acquired at (A) 205 K in toluene-d8 and (B) 190 K in pentane-d12. 1D 1H NMR spectra (red) are overlaid above the 1H projections of the 2D spectra.

90x126mm (300 x 300 DPI)
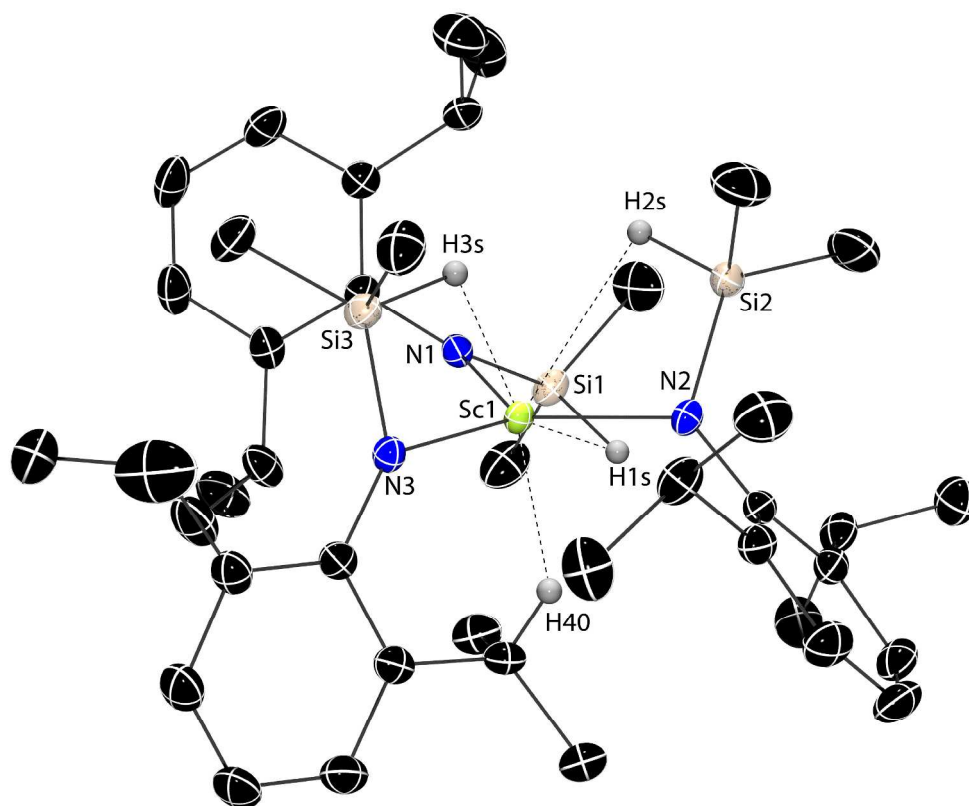
Figure 3. Rendered thermal ellipsoid plot of Sc{N(SiHMe2)Dipp}3 (3) with ellipsoids represented at 50% probability. One of two crystallographically independent molecules is illustrated (see ESI), and the H atoms included in the image are <3 Å from the Sc1 center, are located objectively and included in the refinement.
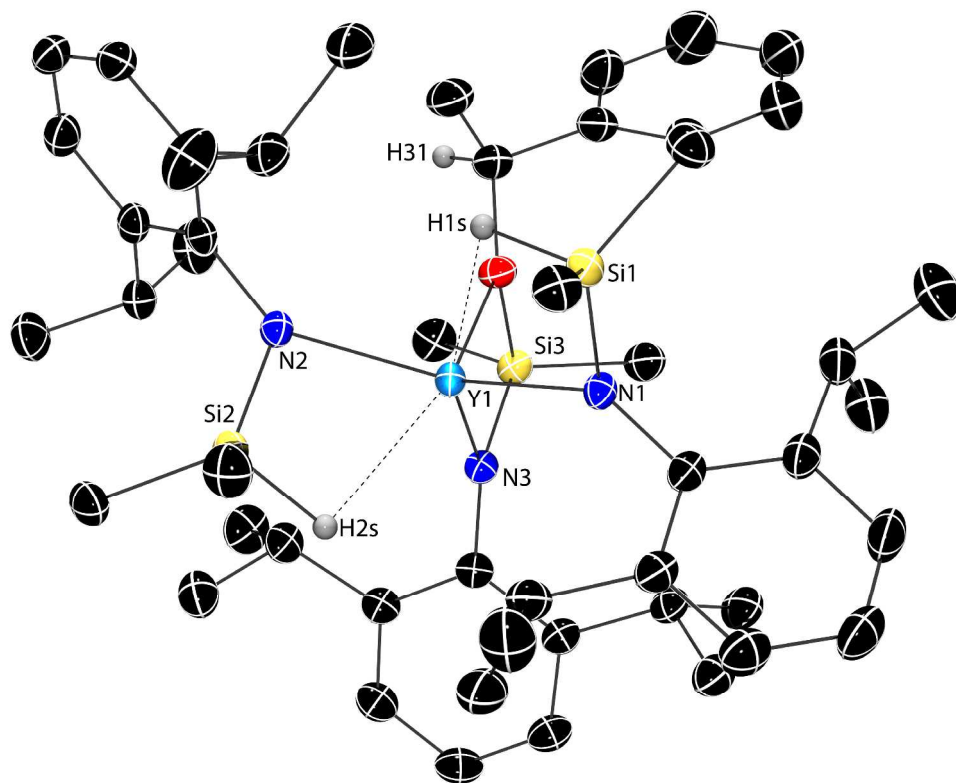
Figure 4. Thermal ellipsoid plot of Y{N(SiMe2OCHMePh)Dipp}{N(SiHMe2)Dipp}2 (6). H atoms bonded to Si were located in the Fourier difference map, refined, and are included in the illustration. H31, which was placed in a calculated position, is included in the image. All other H atoms, crystallographically independent 6, and pentane are not shown for clarity.

Planar, three-coordinate homoleptic rare earth complexes Ln{N(SiHMe$_2$)Dipp}$_3$ (Ln = Sc, Y, Lu), that each contain three secondary Ln←HSi interactions, react with acetophenone via hydrosilylation, rather than by insertion into the Y–N bond or enolate formation.